A NEW JOINT INVERSION ALGORITHM APPLIED TO THE INTERPRETATION OF DC RESISTIVITY AND REFRACTION DATA

T. GÜNTHER[1], L.R. BENTLEY[2] & M. HIRSCH[3]

[1]Leibniz Institute for Applied Geosciences, Hannover, Germany
[2]Department of Geology & Geophysics, University of Calgary, Canada
[3]UFZ Centre for Environmental Research, Leipzig, Germany

Abstract

A new joint inversion algorithm that can be applied to independent physical parameters has been developed. The method allows the interchange of structural information between otherwise independent inversions. It is based on the principles of model-sided robust modeling and the structures in the opposing inversion model are supported, but not strictly enforced. The algorithm uses unstructured meshes that allow the incorporation of topography and other information on the geometry of the subsurface.

A synthetic study is done using refraction tomography and dc resistivity inversion. On one hand it is seen that an existing boundary in one parameter does not enforce the same structure in the other. On the other hand inversion results are significantly improved yielding a clearer separation of units by means of cluster analysis.

The algorithm is applied to the Pine Creek site in Calgary, Alberta, Canada. The site is underlain by approximately 6 m of unsaturated gravel overlying a shaly weathered sandstone bedrock. Repeat profiles using electrical resistivity and seismic refraction were conducted in support of a groundwater study. The joint inversion sharpens the boundaries of the two inversions. It appears to have shifted the boundary to a greater depth. By combining the inversion results with cluster analysis, geologic features are mapped that cannot be seen using individual inversions on their own, reducing the ambiguity of the final stratigraphic model. Improved stratigraphic models will result in an improved ability to model groundwater flow and transport.

1. Introduction

Groundwater flow and transport simulation requires a lot of data to construct and calibrate the model and to assess model performance. Primary data generally comes from drilling logs, coring, water samples, etc. However, these are point measurements and much of the aquifer system is not sampled by the direct methods. Geophysical methods provide spatially dense measurements that can help guide interpolations between the locations of the more directly measured data.

Geophysical measurements are primarily used to characterize the geometry of the hydrostratigraphy or to estimate aquifer properties from the geophysical response with the aid of petrophysical relationships. In both these cases, the use of a single geophysical

technique often leads to non-unique or ambiguous interpretations and estimates. For example, a decrease in electrical resistivity could be due to lower water quality as a result of increasing ion concentration or to a change in lithology from resistive sand to more conductive clay. Similarly, distinguishing between a shaly bedrock and a conductive clay may not be possible using only resistivity.

However, different geophysical properties are sensitive to different porous medium properties. For example, a porous medium's electrical resistivity depends on the resistivity of the pore fluid, the resistivity of the solid matrix, temperature and saturation. Alternatively, seismic wave velocity depends on the bulk and shear moduli and the density of the porous medium. If both a resistivity profile from an electrical resistivity imaging (ERI) survey and a velocity profile from a seismic refraction survey are available, it should be possible to reduce the non-uniqueness associated with using only a single measurement.

Geophysical inversion also suffers from non-uniqueness because limited data causes the inversions to be underdetermined. Regularization, generally in the form of smoothing constraints, is required for unique results. However, smoothing can blur or destroy sharp boundaries. The goal of joint inversion with two geophysical methods is to reduce the severity of smoothing constraints by identifying common structures between the images. Gallardo and Meju (2004) presented a joint inversion method by means of cross-gradients.

In the following, we introduce a robust joint inversion methodology that allows the sharing of structural information between an electrical resistivity inversion and a seismic refraction inversion. We then use cluster analysis to produce an image based on the joint inversion results. The method will be applied to data acquired over a hydrogeologic study site in Calgary, Alberta, Canada.

2. A new joint inversion approach

2.1. **Minimization and Regularization.** Assume D data points d_i subsumed in a data vector $\mathbf{d} = (d_1, \ldots, d_D)$. The parameter distribution $p(\vec{r})$ is discretized by M coefficients m_j yielding model vector $\mathbf{m} = (m_1, \ldots, m_M)$. The vector containing the forward response of a model $\mathbf{m}$ is denoted by $\mathbf{f}(\mathbf{m})$. We try to minimize the discrepancy between data and model response with respect to a certain norm, i.e. the ℓ_2-Norm yielding the method of least squares.

To account for different data accuracy, their standard deviations ϵ_i are used as a weighting function yielding the minimization of

$$\Phi_d(\mathbf{m}) = \sum_{i=1}^{D} \left| \frac{d_i - f_i(\mathbf{m})}{\epsilon_i} \right|^2 = \| \mathbf{D} \left(\mathbf{d} - \mathbf{f}(\mathbf{m}) \right) \|_2^2 \quad \text{with} \quad \mathbf{D} = \mathrm{diag}(1/\epsilon_i) \quad . \tag{1}$$

Beginning from a starting model $\mathbf{m}^0$, a new model $\mathbf{m}^{k+1}$ is obtained by an iterative procedure

$$\mathbf{m}^{k+1} = \mathbf{m}^k + \Delta \mathbf{m}^k \, .$$

We choose the Gauss-Newton algorithm to determine $\Delta \mathbf{m}^k$ due to its fast convergence. Additionally the model has to be constrained to yield a unique solution.

We introduce a model functional Φ_m weighted by a regularization parameter λ

$$\Phi = \Phi_d + \lambda \Phi_m \leftarrow \min \, .$$

To find a general formulation we build a weighted model functional

$$\Phi_m = \|\mathbf{W}_c\mathbf{C}\mathbf{m}\|_2^2 \,. \tag{2}$$

The constraint matrix $\mathbf{C}$ is generally a discrete derivative matrix. The coefficients depend on the element distances and may be varied by the choice of reference points or boundary conditions (2nd order). Generally $\mathbf{C}$ is skewed, i.e. for a 1D parameterization $\mathbf{C} \in R^{(M-1)\times M}$.

The constraint weighting matrix $\mathbf{W}_c$ is generally diagonal $\mathbf{W}_c = \operatorname{diag} w_i^c$. The individual elements w_i^c describe penalty factors for the different model cell boundaries. For example, the model characteristic with respect to horizontal and vertical structures may be controlled. Very small values allow for sharp boundaries which may be identified from boreholes or other methods such as GPR or reflection seismics.

One may use the structure of $\mathbf{m}^k$ to reinforce structures. This procedure is usually applied to data weighting [Claerbout and Muir, 1973] but can also be applied to the model gradients. In fact, the weighting is determined such that an ℓ_1 minimization is simulated which is referred to as robust modeling [Claerbout and Muir, 1973].

Let $\mathbf{c} = \mathbf{C}\mathbf{W}_m(\mathbf{m}-\mathbf{m}^0)$ be the roughness vector. The weighting term w_l^c is determined by the portions of c_l in the ℓ_1 and ℓ_2-Norm

$$w_l^c = \frac{\frac{|c_l|^1}{\|\mathbf{c}\|_1^1}}{\frac{|c_l|^2}{\|\mathbf{c}\|_2^2}} = \frac{\frac{|c_l|}{\sum |c_i|}}{\frac{c_l^2}{\sum c_i^2}} = \frac{\sum c_i^2}{|c_l| \sum |c_i|} \quad . \tag{3}$$

To avoid enforcement of strong contrasts, all $w_l^c > 1$ are set to 1. Thus, we obtain models with more contrast by introducing an additional non-linearity.

2.2. **The new approach.** Instead of using the structure of $\mathbf{m}^k$ for $\mathbf{m}^{k+1}$, we apply the latter procedure to introduce structural information to a parameter vector $\mathbf{p}$. Thus, the weights w_l^c for determining $\mathbf{p}^{k+1}$ are calculated after (3) from $\mathbf{c} = \mathbf{C}\mathbf{W}^c(\mathbf{m}^k - \mathbf{m}^0)$. Simultaneously, the gradients of $\mathbf{p}^k$ are used to obtain the constraint weights for $\mathbf{m}^{k+1}$.

The joint inversion scheme is illustrated in Figure 1 for DC and refraction tomography.

From both data sets a mesh incorporating topographical information is created. Electrode positions and geophones/shotpoints must be included as node points. Then we choose a starting resistivity model ρ_0 and velocity model v_0. An appropriate constraint matrix $\mathbf{C}$ is created which is used to derive the first iteration models ρ_1 and v_1 independently.

In the next step the resistivity model rho1 is used to alter the smoothness matrix used for velocity inversion, $\mathbf{C}_v$. Analogously, the smoothness matrix $\mathbf{C}_\rho$ for resistivity inversion is built up based on the velocity. Thus, structural information is exchanged through the smoothness matrices. We continue the sequential iterations with updated smoothness matrices until convergence to the final models ρ_n and v_n.

Finally, a cluster algorithm is used to find a model that combines both parameters. Both inversion parameters are input into the cluster algorithm. Additionally, the geometric position of the cell, i.e. x and z of the midpoint, is used to find contiguous clusters. In our experience, clustering based on euclidean distances and complete linkage provided appropriate results.

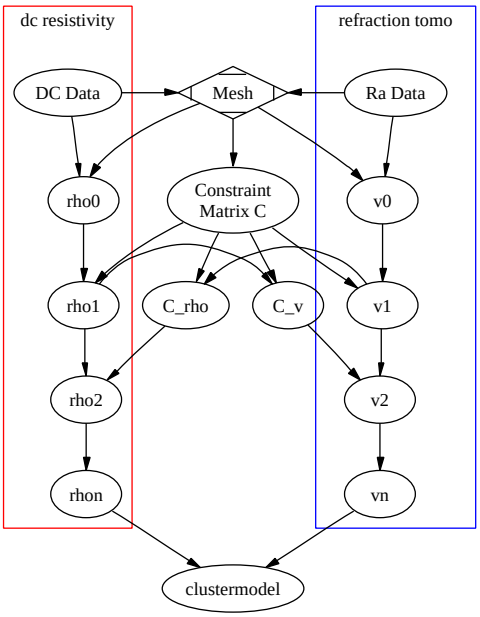

FIGURE 1. Scheme of the joint inversion procedure for combined dc resistivity and refraction tomography

For the resistivity method, the data were the logarithm of the apparent resistivities, and the model parameters were the logarithm of the cell resistivities to ensure positivity. For the forward operator and the sensitivity calculation the techniques of [Günther and Rücker, 2005] have been applied.

The refraction data are first arrival travel times. The model parameters are the logarithm of velocities. To solve the forward problem we used a Shortest Path algorithm [Dijkstra, 1959] that restricts the ray paths to the model edges. Although this is only accurate for very fine meshes, it is sufficient to prove the concept.

3. Synthetic Study

We now test the technique with a sophisticated model. At first we introduce a slope connecting two different levels. Triangular meshes are used to discretize the model parameters. Figure 2 shows the synthetic model used for creating the data. It consists of two layers with an additional unit in-between. Its velocity equals that of the upper layer, whereas the resistivity is identical to the one of the lower layer. Thus, both common and different boundaries exist around the red block.

We assumed 41 electrodes/geophones with 1 m spacing between -15 and 25 m. A complete Wenner pseudo-section was applied to create the dc data. For the refraction data every 5th geophone was used as a shot point with receivers at the other locations. Synthetic data have been created using a highly refined quality model to avoid errors. Additionally Gaussian errors of 3% (for dc data) and 0.5 ms (Ra data) standard deviation were added.

The inversion has been carried out once without and once with coupling. In Figure 3 the inversion results are displayed for separate (left) and joint (right) inversion. Both methods

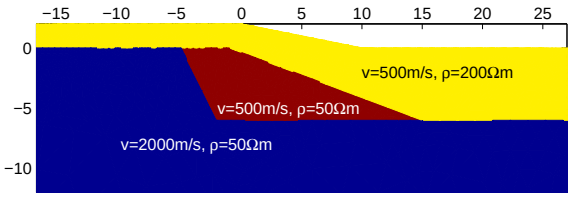

FIGURE 2. Synthetic model with three units consisting of 2 different velocities and resistivities.

show the different structures of their synthetic models in the separate inversion. In the separate inversions, gradients are smooth due to the smoothness constraints, especially near the boundaries. The resolution of the resistivity data is too low at depth to resolve the resistive bedrock well.

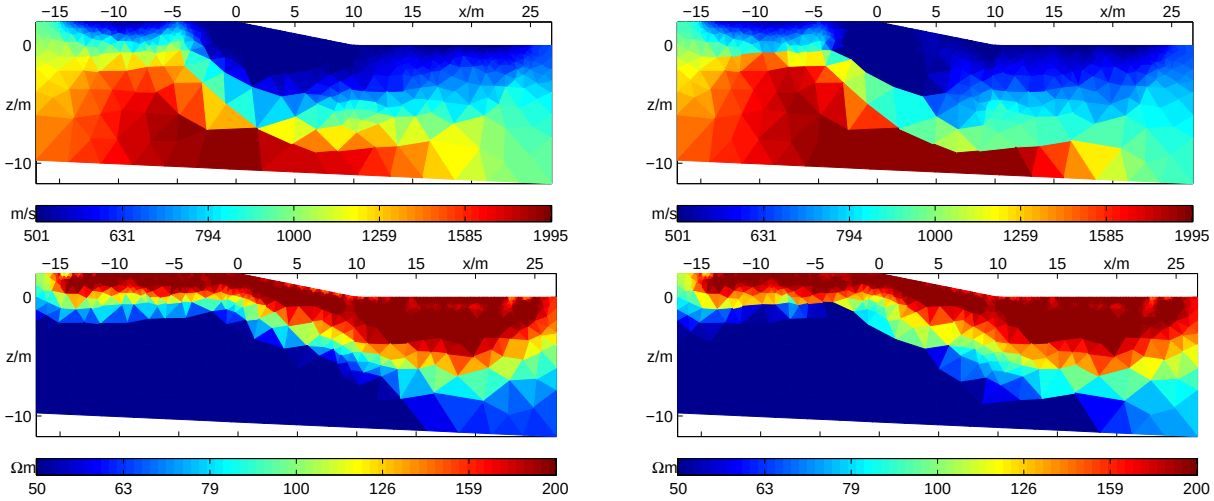

FIGURE 3. Inversion results (velocity on top, resistivity at bottom) for the synthetic model of Fig. 2 for separate inversion (left) and joint inversion (right)

Using the joint inversion (right hand side), the gradients become much sharper where resistivity and velocity have identical boundaries. At the single boundaries the gradients remain smooth and phantom model boundaries from one parameter are not projected into the other parameter. In regions of missing resolution, as the right boundary, the joint inversion cannot improve the results.

A final image of the combined inversion is obtained using cluster analysis. We used Chebychev (interior) distances and an average linkage method and restricted the number of clusters to 3 as in the synthetic model. Figure 4 displays the final model.

Clearly the upper layer can be traced, and the parameters coincide very well with the synthetic model (Figure 2). Similarly the lower boundary layer is well defined, although their velocity is underestimated. The intermediate block matches quite well with the synthetic model in the central part. However, both velocity and resistivity are overestimated. Near the right boundary the resolution is too low at depth to image the course of the layer boundary well.

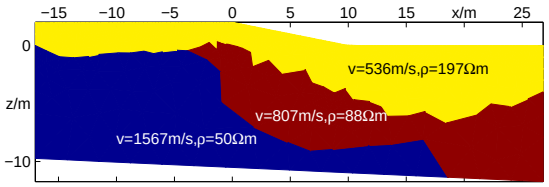

FIGURE 4. Final model obtained by cluster analysis of the joint inversion velocity and resistivity results.

4. STUDY SITE

4.1. **Site description.** The Pine Creek field site is located on a terrace adjacent to the Bow River in south Calgary, Alberta Canada (Figure 5). The field site is underlain by sand, gravel, and fine grained sediments that overlie shaly sandstone bedrock. The bedrock surface is uneven and contains the remnants of channel morphology. Depth to bedrock ranges between 2.5 and 8.5 m. In the west the terrace is bounded by a steep valley slope consisting of lake bed sediments overlying bedrock. In the East, the terrace is bounded by the steep slope at the margin of the present Bow River channel. The water table is in the gravels within the paleochannels, but is within the bedrock in the regions of bedrock high. Detailed knowledge of the location and depth of the channels, location of the water table, thickness of gravel and location of fine grained deposits were needed in order to analyze whether the terrace gravels could produce enough water to supply artificial streams a proposed experimental site.

Three ERI lines were conducted and subsequently repeated with refraction surveys. Due to space limitations we will only present the results from the southwest end of Line 1 (Figure 5). In addition, several boreholes were located along the line and the borehole logs can be used for evaluating the performance of the algorithms. The ERI equipment had 56 electrodes and data was collected using a Wenner array. The line was run with 2 m unit electrode spacing and then repeated with 4 m unit electrode. Lines were extended by sequentially rolling the 14 electrode cables to the front of the line. A 60 channel seismic system was used to collect the seismic refraction data. Geophones were spaced every 2 m and the line was advanced by moving 30 channels at a time. Stacked sledge hammer on plate blows were used as the energy source.

4.2. **Results.** As for the synthetic model, the inversions are carried out separately and jointly. Figure 6 shows the individual results. The cells without ray coverage are blanked out leaving a discontinuous image. Throughout the model we see faster velocities below a locally interrupted low-velocity zone at the surface. The slowest values occur around the shot points, and are apparently inversion artifacts. Velocities of 3000-4000 correspond to the unweathered bedrock.

The resistivity shows a good conductor at depth under a resistive coverage. The low resistivity correlates with the conductive shaly bedrock. In both methods a change in character is seen at 20-40 m due to a change from gravel to fine-grained associated with the valley wall. As in the velocity model the transitions are smooth. In contrast, the model obtained by joint inversion contains similar features, but the image boundaries are sharper. The parameter boundaries in the two joint inversion images are more consistent

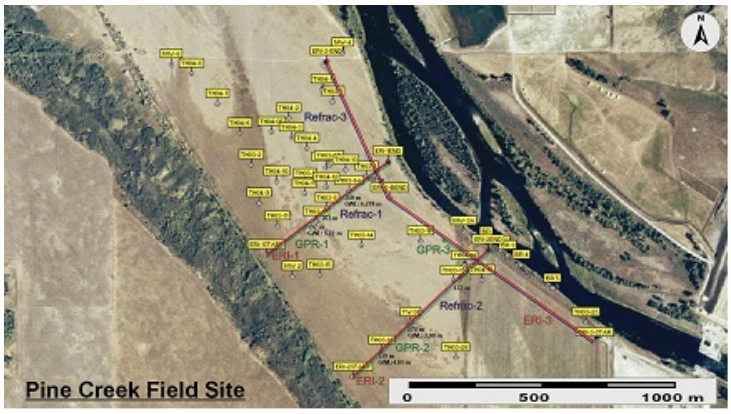

FIGURE 5. Site map with location of Line 1 highlighted

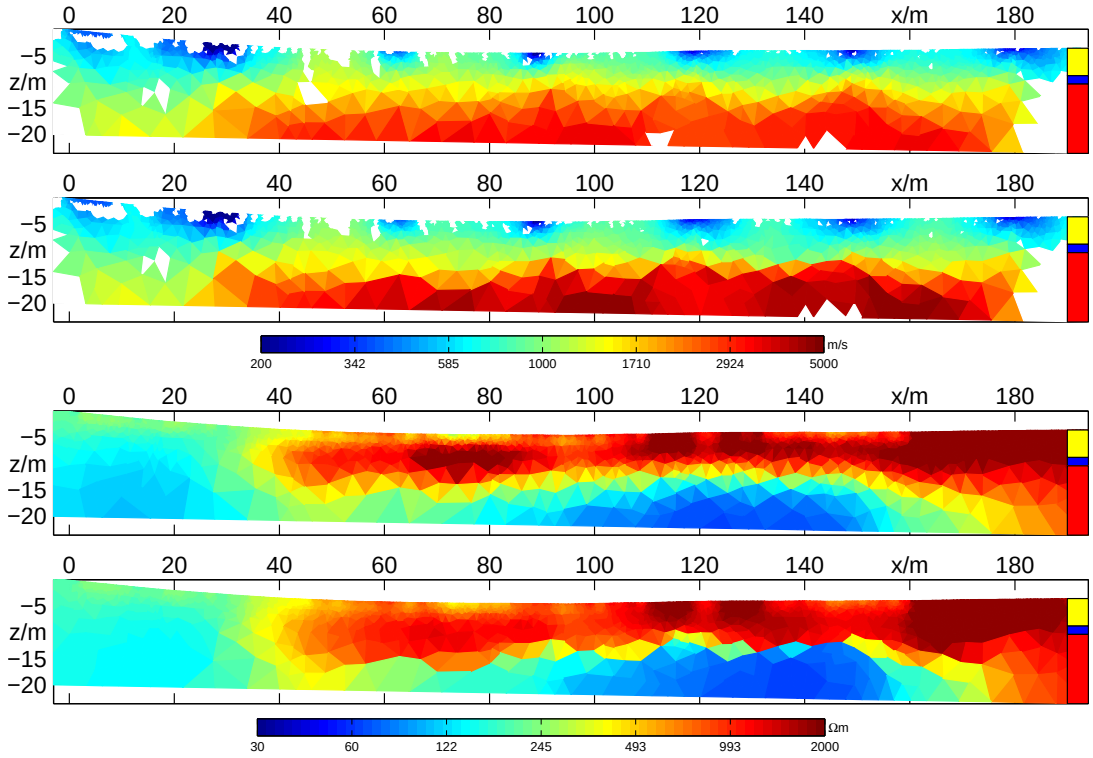

FIGURE 6. Inversion results (velocity on top, resistivity at bottom) for the field data of Fig. 2 for separate inversion and joint inversion

than in the separate inversion boundaries, especially in the east. At the very west the structures are still unclear, since the resolution is low. However, the boundaries appear deeper in comparison with the separate inversion results.

Finally, Figure 7 displays the cluster solution using four clusters. The image is consistent with a gravel layer overlying a shale bedrock in the east. Both images show that the gravel grades into the higher conductivity, lower velocity lake bed silts of the valley wall, which are also underlain by the shale bedrock. The transition from gravel to silt is

clear in the resistivity inversion, but the position of the underlying bedrock is not evident. In contrast, the transition to silt is not evident on the refraction line, but there is some evidence of the bedrock interface. By combining the two data sets in the cluster analysis, both the gravel-silt transition and the position of the underlying bedrock are evident. On the other hand, the one point with well control appears to indicate that the joint inversion gravel-bedrock interface has been shifted too deep.

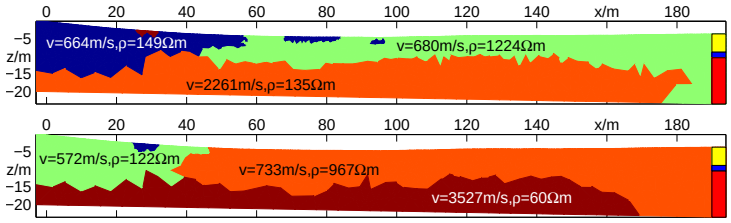

FIGURE 7. Final cluster model of the separately (upper) and jointly (lower) inverted parameters by a restriction to four clusters

5. Conclusion

We presented a new joint inversion algorithm that combines different data by structural coupling between otherwise independent tomographic inversions. It is based on the ideas of robust modeling and produces clearer images of the subsurface. However, it does not enforce structures that do not agree with the data. A cluster analysis can be used to yield a conceptional image of the subsurface.

In regions of missing resolution the joint inversion cannot, of course, improve the results. It is only able to reduce the ambiguities. If fuzzy cluster analysis is performed, it may be possible to obtain measures of reliability for both image resolution and cluster analysis. Application of fuzzy cluster analysis remains an area of future work.

The method has been tested on dc resistivity and seismic refraction data from the Pine Creek site. The joint inversion method increased the sharpness of the surficial sediment-bedrock boundary. However, it may have caused the boundary to be imaged too deep. We are working on improving the weighting strategy to address this issue. Cluster analysis was used to combine the two results into one image. The combined cluster images captured aspects of the geology that could not be imaged using only one method.

References

Claerbout and Muir, 1973. Claerbout, J. F. and Muir, F. (1973). Robust modeling with erratic data. *Geophysics*, 38(1):826–844.

Dijkstra, 1959. Dijkstra, E. W. (1959). A note on two problems in connexion with graphs. *Numerical Mathematics*, 1:269–271.

Gallardo and Meju, 2004. Gallardo, L. A. and Meju, M. A. (2004). Joint two-dimensional dc resistivity and seismic travel time inversion with cross-gradients constraints. *J. Geophys. Res.*, 109:03311.

Günther and Rücker, 2005. Günther, T. and Rücker, C. (2005). A triple-grid technique for the 3d inversion of dc resistivity data incorporating arbitrary topography. In *EAGE Near Surface Conference*, Palermo, Italy.

Vozoff and Jupp, 1975. Vozoff, K. and Jupp, D. L. B. (1975). Joint inversion of geophysical data. *Geoph. J. R. astr. Soc.*, 42:977–991.